

# $J/\psi$ production in p-A and A-A collisions at fixed target experiments

Roberta Arnaldi<sup>a</sup> for the NA60 Collaboration

<sup>a</sup>INFN Torino, Via P. Giuria 1, Torino, I-10125, Italy

---

## Abstract

Charmonia suppression is one of the main signatures for the formation of a deconfined medium. However, also nuclear effects, not related to the production of a hot medium, can affect the  $J/\psi$  yield. The determination, from the study of p-A collisions, of the  $J/\psi$  behaviour in nuclear matter is, therefore, extremely important to correctly quantify the amount of charmonia suppression induced by the deconfined medium. In this paper the new NA60 results collected at 158 GeV incident energy, i.e. under the same kinematical conditions as the In-In (NA60) and Pb-Pb (NA50) data, are presented and compared with p-A measurements from other fixed target experiments. Results on A-A collisions are also reviewed taking into account the new available information on the influence of cold nuclear matter on the  $J/\psi$  production yield. Finally, results on the  $J/\psi$  polarization are shown for p-A and A-A collisions.

---

## 1. Introduction

$J/\psi$  suppression in A-A collisions is considered to be one of the main signatures for the phase transition from an hadronic to a deconfined medium [1]. However, the  $J/\psi$  production can be affected also by cold nuclear matter effects, as, for example, the final state absorption of the  $c\bar{c}$  pair in the nuclear medium, the parton shadowing or the initial and final state energy loss. The amplitude of these effects, not related to the formation of a deconfined medium, is determined from p-A collisions and then extrapolated to A-A interactions to be compared with the measured  $J/\psi$  yield.

At SPS energies, cold nuclear matter effects are usually parameterized, in the frame of the Glauber model, by fitting the A-dependence of the  $J/\psi$  production cross section per nucleon-nucleon collision. These nuclear effects are quantified through the value of  $\sigma_{abs}^{J/\psi}$  extracted, up to now, from the NA50 data at 400/450 GeV ( $\sigma_{abs}^{J/\psi} = 4.2 \pm 0.5$  mb) [2]. Another way to parameterize cold nuclear matter effects is based on a fit to the A-dependence of the  $J/\psi$  production cross section using a  $A^\alpha$  power law. A value of  $\alpha$  different from unity indicates how much the  $J/\psi$  yield is modified by the nuclear medium. It should be noted that both  $\alpha$  and  $\sigma_{abs}^{J/\psi}$  are effective quantities, since they represent the amount of cold nuclear matter effects reducing the  $J/\psi$  yield, but they do not allow to disentangle the different contributions (e.g. shadowing, nuclear absorption) playing a role in this reduction. Nuclear effects, evaluated from p-A data at 400/450 GeV, are then extrapolated to A-A collisions at a lower energy (158A GeV) assuming in both cases a scaling with L, the mean thickness of nuclear matter seen by the  $c\bar{c}$  pair in its way out through the nucleus, and imposing  $\sigma_{abs}^{J/\psi}$  to be energy independent. The expected  $J/\psi$  yield is then compared with the measured one, as a function of centrality. Following the aforementioned approach, a

23 further suppression (the so called “anomalous”  $J/\psi$  suppression), exceeding cold nuclear matter  
24 effects, is indeed observed at SPS in Pb-Pb [3] and In-In [4] collisions. It is clear that to correctly  
25 quantify the amount of suppression due to the formation of a hot medium, the  $J/\psi$  behaviour in  
26 the normal nuclear matter must be determined with high precision.

27 Several results on  $J/\psi$  production in p-A collisions at fixed target experiments are available,  
28 covering different kinematic and energy domains. HERA-B at HERA, for example, has studied  
29 p-Cu, Ti, W reactions at 920 GeV [5], E866 at FNAL p-Be, Fe, W collisions at 800 GeV [6],  
30 NA50 at SPS proton induced collisions on several nuclei (Be, Al, Cu, Ag, W, Pb) at 400/450  
31 GeV [2] and finally NA3 at SPS p-H<sub>2</sub>, Pt collisions at 200 GeV [7]. It is important to note that  
32 none of these existing results has been obtained under the same conditions, in terms of energy and  
33 kinematic domain, as the SPS A-A collisions collected at 158A GeV. This implies that several  
34 assumptions (as the energy independence of  $\sigma_{abs}^{J/\psi}$ ) had to be done, in order to extrapolate cold  
35 nuclear matter effects from p-A to A-A collisions.

## 36 2. NA60 p-A results

37 For the first time the NA60 experiment has studied the  $J/\psi$  production in p-A collisions at  
38 158 GeV [8], in order to provide a reference collected under the same kinematic and energy  
39 conditions as the A-A data.

40 The experimental apparatus of NA60 is based on a traditional muon spectrometer coupled  
41 with a vertex telescope made of Si pixel planes, close to the target region. The matching, based on  
42 the tracks coordinates and momentum between the tracks reconstructed in the two spectrometers,  
43 allows an accurate measurement of the muon kinematics and therefore an improvement in the  
44 quality of the results with respect to previous experiments. For details on the apparatus see [9].  
45 The target system of NA60, during the p-A data taking, was based on 7 different targets (Be, Al,  
46 Cu, In, W, Pb, U) simultaneously exposed to the beam. NA60 has also collected data at 400 GeV,  
47 with the same experimental setup as the one of the 158 GeV data taking period, to be used as a  
48 cross-check of the NA50 results taken at the same energy.

### 49 2.1. $J/\psi$ kinematical distributions

50 The investigation of the  $J/\psi$  kinematical distributions may help to obtain further insights in  
51 the understanding of the charmonium production and initial state effects. In Fig.1 the rapidity  
52 ( $y_{CM}$ ) distributions corresponding to p-A collisions at 158 GeV and 400 GeV are shown. A 1-D  
53 acceptance correction has been performed assuming realistic transverse momentum distributions  
54 and a flat  $\cos\theta_{CS}$  shape (see Sec.4 for this definition). Within the narrow rapidity coverage  
55 of NA60 (one rapidity unit), the distributions can be reproduced by a Gaussian function. A  
56 simultaneous fit to the distributions corresponding to the different p-A collisions indicates that,  
57 at 158 GeV, the data can be described by a gaussian centered at midrapidity ( $\mu_y = 0.05 \pm 0.05$ )  
58 with a width  $\sigma_y = 0.51 \pm 0.02$ . At 400 GeV, because of the wider distributions, the peak position  
59 is less constrained. In this case the fit is performed imposing the slightly negative mean value  
60 ( $\mu_y = -0.2$ ) measured by NA50 with a high statistics data set at the same energy [2]. As expected,  
61 because of the higher energy, a larger rapidity width ( $\sigma_y = 0.81 \pm 0.03$ ) is obtained, in agreement,  
62 within errors with the NA50 value ( $\sigma_y \sim 0.85$ ). Unfortunately, the precision of these results do  
63 not allow to investigate the negative rapidity shift observed by NA50, neither to confirm the  
64 smaller A-dependent shift of the center of the  $x_F$  (and therefore  $y$ ) distributions observed by  
65 HERA-B [5].

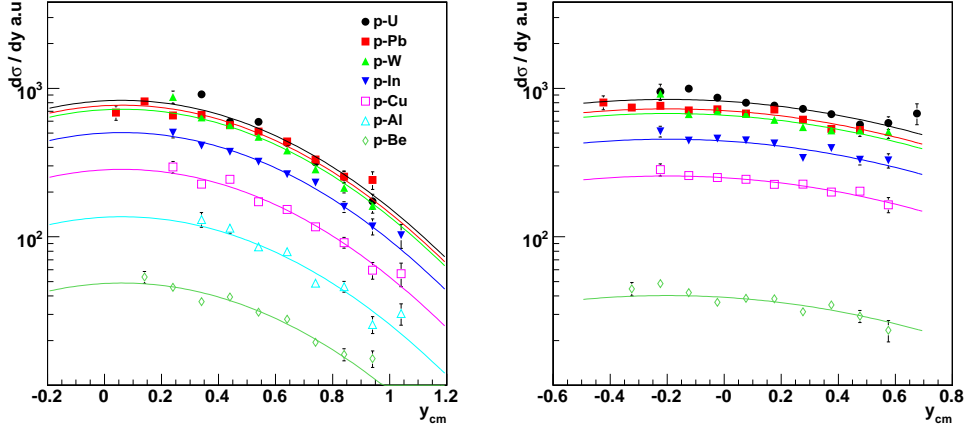


Figure 1:  $J/\psi$  acceptance corrected rapidity distributions at 158 GeV (left) and 400 GeV(right).

66 The  $J/\psi$  transverse momentum ( $p_T$ ) distributions have also been studied. The spectra are  
67 corrected with an 1-D acceptance, obtained assuming a flat  $p_T$  distribution and realistic  $y$  and  
68  $\cos\theta_{CS}$  shapes. A broadening of the  $p_T$  distributions as a function of  $A$  is measured at both  
69 158 and 400 GeV. This confirms previous observations from other experiments [5, 7, 10, 11,  
70 12, 13, 14] and is usually interpreted as initial state multiple scattering of the incoming gluons  
71 (Cronin effect) before the hard scattering which will produce the  $c\bar{c}$  pair. The average  $\langle p_T^2 \rangle$   
72 dependence on the mass number can be parameterized with  $\langle p_T^2 \rangle = \langle p_T^2 \rangle_{pp} + \rho(A^{1/3} - 1)$  [5],  
73 where  $A^{1/3} - 1$  is roughly proportional to the length  $L$ . As shown in Fig.2 (left) the  $\langle p_T^2 \rangle_{pp}$   
74 values are compatible with a linear growth with the square of the center of mass energy  $s$ . On  
75 the other hand, the slope of the parameterization  $\rho$  shows an almost energy independent pattern,  
76 apart from a hint of decrease at low energy, corresponding to the NA60 158 GeV result.

## 77 2.2. Cold nuclear matter effects

78 New NA60 results on the nuclear effects affecting the  $J/\psi$  at 158 GeV have been presented  
79 at this conference [8]. Results, integrated over the full  $p_T$  range are given in the rapidity region,  
80 covered by all the subtargets, corresponding to  $0.28 < y_{CM} < 0.78$ . Nuclear effects are evaluated  
81 comparing the cross section ratio,  $\sigma_{pA}^{J/\psi} / \sigma_{pBe}^{J/\psi}$ , between the target with mass number  $A$  and the  
82 lightest one (Be). By computing this ratio, the beam luminosity factors cancel out, apart from a  
83 small beam attenuation factor. However, since the sub-targets see the vertex telescope under a  
84 slightly different angle, the track reconstruction efficiencies do not completely cancel out. There-  
85 fore an accurate evaluation of such quantities and their time evolution has been performed target  
86 by target, with high granularity down to the single pixel level, and on a run-per-run basis.

87  $J/\psi$  cross-section ratios are shown in Fig.2 (right) as a function of  $L$ . In the same figure, also  
88 results from a similar analysis performed on the 400 GeV data sample are shown. In this case, the  
89 results refer to the kinematical region  $-0.17 < y_{CM} < 0.33$ , corresponding to the same rapidity  
90 range, in the laboratory frame, as the 158 GeV one. Systematic errors include uncertainties on the  
91 target thickness, on the  $y$  distribution used in the acceptance calculation and on the reconstruction

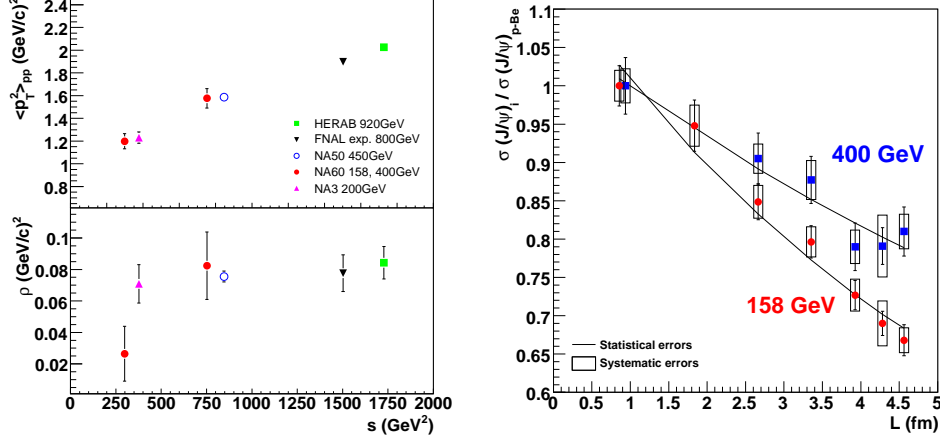


Figure 2: Left: energy dependence of the  $\langle p_T^2 \rangle_{pp}$  (top) and  $\rho$  (bottom) parameters. Right:  $J/\psi$  cross section ratios for p-A collisions at 158 GeV (circles) and 400 GeV (squares), as a function of  $L$ .

92 efficiency. Only the fraction of systematic error, not in common to all the points, is shown, since  
 93 it is the one affecting the evaluation of the nuclear effects.

94 Performing a Glauber fit to the data, or using the  $\alpha$  parameterization, the following results  
 95 are obtained for the new NA60 p-A data:  $\sigma_{abs}^{J/\psi} = 7.6 \pm 0.7$  (stat.)  $\pm 0.6$  (syst.) mb ( $\alpha = 0.882$   
 96  $\pm 0.009 \pm 0.008$ ) at 158 GeV and  $\sigma_{abs}^{J/\psi} = 4.3 \pm 0.8$  (stat.)  $\pm 0.6$  (syst.) mb ( $\alpha = 0.927 \pm 0.013$   
 97  $\pm 0.009$ ) at 400 GeV. It has to be stressed out that the  $\sigma_{abs}^{J/\psi}$  result at 400 GeV is smaller with  
 98 respect to the one extracted from the 158 GeV, pointing to an energy dependence of this quantity.  
 99 Furthermore, the obtained value is in very good agreement with a previous result obtained by  
 100 NA50 at the same energy [2].

101 The comparison with results from previous experiments (HERA-B, E866 and NA50) can be  
 102 done in terms of the extracted  $\alpha$  [8] or  $\sigma_{abs}^{J/\psi}$  values, as a function of the Feynman  $x_F$  variable ( $x_F$ ). As  
 103 shown in Fig.3 (left), where all the available measurements are compared, a strong dependence  
 104 of  $\sigma_{abs}^{J/\psi}$  on  $x_F$  and on the beam energy is clearly visible. Cold nuclear matter effects are stronger  
 105 at high  $x_F$  and for a fixed  $x_F$  value their importance increases while lowering the beam energy.  
 106 As shown in the figure, the new NA60 results at 400 GeV confirm the NA50 values obtained at  
 107 a similar energy. On the other hand, the 158 GeV data seem to point to higher  $\sigma_{abs}^{J/\psi}$  values, with  
 108 a hint for an increase in the narrow explored  $x_F$  region. It is also worthwhile to note that older  
 109 NA3 results [7] on  $J/\psi$  production are in partial contradiction with these observations, showing  
 110 lower  $\sigma_{abs}^{J/\psi}$  values, rather similar to those obtained with the higher energy data samples.

111 Although not shown here, the results do not present any scaling with  $x_2$ , the fraction of  
 112 nucleon momentum carried by the target colliding partons. Since  $x_2$  is the variable driving the  
 113 shadowing effects, the break of this scaling confirms the fact that parton shadowing can not be  
 114 the only mechanism invoked to describe the data. It is, therefore, clear that the interpretation  
 115 of the kinematical dependence of the cold nuclear matter effects is extremely complicated since  
 116 there are many competing mechanisms affecting the  $J/\psi$  production and propagation into the  
 117 nuclei. A theoretical description of the cold nuclear matter effects over the full kinematic range  
 118 is extremely complex and not yet available [15, 16, 17].

119 As discussed, the  $\alpha$  or the  $\sigma_{abs}^{J/\psi}$  values are effective quantities used to describe the convolution  
 120 of all the cold nuclear effects not related to the formation of a deconfined medium. At this confer-  
 121 ence, a first attempt to take explicitly into account the parton shadowing contribution to the  
 122 NA60 data has been proposed. It must be noted that at SPS energies, the charmonia production  
 123 explores a range of  $x$  (the fraction of the nucleon momentum carried by the parton) correspond-  
 124 ing to the antishadowing region, where parton densities in the nuclei are enhanced with respect to  
 125 those of the free nucleons. The antishadowing, evaluated with the EKS98[18] parameterization  
 126 for the nuclear modification of the parton distribution functions (PDF), causes an enhancement  
 127 of the charmonium production cross section per nucleon-nucleon collision. Therefore, if this  
 128 initial-state contribution is explicitly taken into account, a larger  $\sigma_{abs}^{J/\psi}$  value is needed to de-  
 129 scribe the measured data ( $\sigma_{abs}^{J/\psi}(158\text{GeV}) = 9.3 \pm 0.7 \pm 0.7$  mb and  $\sigma_{abs}^{J/\psi}(400\text{GeV}) = 6.0 \pm 0.9 \pm 0.7$   
 130 mb). Results depend on the adopted parameterization of the PDF nuclear modifications. Slightly  
 131 higher  $\sigma_{abs}^{J/\psi}$  values ( $\sim 5 - 10\%$ ), for example, are obtained if the EPS08 [19] parameterization is  
 132 used.

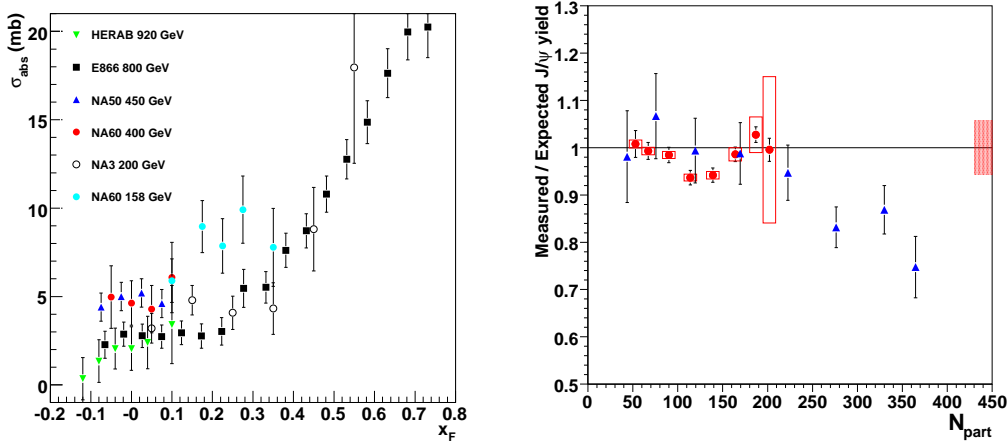


Figure 3: Left: Compilation of  $\sigma_{abs}^{J/\psi}$  values versus  $x_F$ . Right:  $J/\psi$  suppression pattern in In-In (circles) and Pb-Pb (triangles). Boxes around the points correspond to the correlated systematic errors, while the filled box on the right is the uncertainty on the absolute normalization of the In-In points. A further global 12% error, not shown, is due to the uncertainty on  $\sigma_{abs}^{J/\psi}$ .

### 133 3. Anomalous $J/\psi$ suppression in In-In and Pb-Pb collisions

134 As previously discussed, the cold nuclear matter reference used up to now for A-A collisions  
 135 by NA50 [3] and NA60 [4] was based on the  $\sigma_{abs}^{J/\psi}$  value obtained from p-A collisions at 400/450  
 136 GeV, assuming  $\sigma_{abs}^{J/\psi}$  to be independent of the incident energy and  $y_{CM}$  range. As shown in Fig.3  
 137 (left), this is not the case, since the cold nuclear matter effects strongly depends on the energy and  
 138 kinematical domain. Therefore the evaluation of the size of the effects affecting A-A collisions at  
 139 158A GeV must be based on the new p-A NA60 results at the same energy. The expected shape  
 140 for the  $J/\psi$  distribution in cold nuclear matter is computed within a Glauber model, assuming  
 141 the  $J/\psi$  production as a function of centrality (determined measuring the energy,  $E_{ZDC}$ , released

142 in a Zero Degree Calorimeter)  $dN_{J/\psi}^{exp}/dE_{ZDC}$  to scale with the number of binary collisions. The  
 143 nuclear effects affecting the  $J/\psi$  are then implemented assuming  $\sigma_{abs}^{J/\psi} = 7.6 \pm 0.7 \pm 0.6$  mb, as  
 144 discussed in the previous section. This reference curve is then compared with the measured In-In  
 145  $dN_{J/\psi}^{meas}/dE_{ZDC}$  distribution, following the procedure described in [4]. As expected, since the  
 146  $\sigma_{abs}^{J/\psi}$  value directly obtained at 158 GeV is higher than the one extracted from p-A data at 400/450  
 147 GeV, the amount of anomalous suppression will be smaller with respect to the previous estimates.  
 148 Furthermore, in the procedure followed up to now to build the reference curve, shadowing effects  
 149 were not explicitly taken into account. While in p-A data only partons in the target are affected  
 150 by shadowing, in A-A collisions also the projectile is involved and this further contribution has  
 151 to be included when extrapolating the cold nuclear effects from p-A to A-A [20]. It turns out  
 152 that if the shadowing is neglected in this extrapolation, a small bias is introduced, resulting in a  
 153  $\sim 5\%$  artificial contribution to the suppression of the  $J/\psi$  yield (if the EKS98 parameterization is  
 154 used for the shadowing evaluation). Therefore, if shadowing is properly taken into account in the  
 155 extrapolation from p-A to A-A, a further reduction of the  $J/\psi$  suppression is observed. This is  
 156 shown in Fig.3 (right), where the final ratio of the measured and expected  $J/\psi$  yield is presented  
 157 as a function of the number of participants ( $N_{part}$ ) for both In-In and Pb-Pb data. Even within  
 158 this new definition of the reference curve, for very central Pb-Pb collisions ( $N_{part} > 200$ ) an  
 159 anomalous  $J/\psi$  suppression, of the order of 20-30%, is still visible.

#### 160 4. $J/\psi$ polarization

161 The measurement of the  $J/\psi$  polarization is an important tool to clarify the quarkonium  
 162 production mechanism, since different theoretical models predict different degree of polariza-  
 163 tion [21]. For example, polarization is expected to be sensitive to the spin states of the  $c\bar{c}$   
 164 pair [22], therefore its measurement can shed some light on the color-singlet and color-octet  
 165 contributions to the production process. Contrary to other observables, as the differential cross-  
 166 sections, in the polarization predictions uncertainties related to the theoretical inputs cancel out,  
 167 therefore providing well-defined expected values. However, quarkonium polarization has always  
 168 represented a puzzle, since, at collider experiments, the theoretical models, which were able  
 169 to predict the observed  $J/\psi$  production cross section, clearly failed in the description of the  $p_T$   
 170 dependence of the polarization [23].

171 Experimentally, the  $J/\psi$  polarization is measured from the full angular distribution of the  
 172 quarkonium decay products:

$$\frac{dN}{d\cos\theta d\phi} = 1 + \lambda \cos^2\theta + \mu \sin 2\theta \cos\phi + \frac{\nu}{2} \sin^2\theta \cos 2\phi \quad (1)$$

173 where the polar angle  $\theta$  is determined by the direction of the positive muon, in the quarkonium  
 174 rest frame, and a chosen  $\vec{z}$  polarization axis (defining the decay plane).  $\phi$  is the azimuthal angle  
 175 between the reaction plane, containing the colliding hadrons and the decay plane. The  $\lambda$  param-  
 176 eter is traditionally called ‘‘polarization’’: zero value for  $\lambda$  indicates that the  $J/\psi$  are not polarized,  
 177 while  $\lambda=1(-1)$  means transverse (longitudinal) polarization. Non zero values of  $\mu$  and  $\nu$  indicate  
 178 an azimuthal anisotropy of the distributions.  $\lambda$ ,  $\mu$  and  $\nu$  depend on the chosen definition of the  
 179  $\vec{z}$  axis. It is, therefore, useful, to determine these parameters in more than one reference frame.  
 180 However, it can be noted that the knowledge of the full set of coefficients allows to analytically  
 181 calculate their values in other frames, through appropriate transformations and knowing the  $J/\psi$

182 kinematics [24]. Of course, this is not the case if only the  $\lambda$  parameter is measured. In the litera-  
 183 ture the most commonly used frames are the Collins-Soper (CS) one, where the  $\vec{z}$  axis is parallel  
 184 to the bisector of the angle between the projectile and target directions in the  $J/\psi$  rest frame, and  
 185 the helicity (HE) one, where the  $\vec{z}$  axis coincides with the quarkonium direction in the target-  
 186 projectile center of mass frame. It is important to note that because of the  $\lambda$ ,  $\mu$  and  $\nu$  dependence  
 187 on a chosen reference frame, polarization results from different experiments can be compared  
 188 only if the same frame is adopted. Most previous polarization analyses up to now were limited  
 189 to the choice of only one specific reference frame and were restricted to the measurement of the  
 190 polar angle distribution. On the contrary, recent results from HERA-B [25] and NA60 [8] have  
 191 been obtained measuring for the first time the full angular distribution of the decay products of  
 192 charmonia and comparing different frames.

193 NA60 results are obtained applying a 1-D acceptance correction, assuming realistic  $y_{\text{CM}}$  and  
 194  $p_T$  distributions and a flat  $\cos\theta$  and  $\phi$  spectra. The measured polarization values present a de-  
 195 pendence on the  $J/\psi$  transverse momentum, as shown in Fig.4 (left) for the helicity frame. In  
 196 particular, HERA-B  $\lambda$  results indicate an increase of the  $J/\psi$  polarization, moving from slightly  
 197 negative values (corresponding to longitudinal polarization) at low  $p_T$  to values close to zero  
 198 (absence of polarization) at higher  $p_T$ . The first polarization results obtained in p-A collisions at  
 199 158 GeV and 400 GeV by the NA60 experiment confirm, within errors, the observed trend.

200 In Fig.4 (left) results on the the azimuthal parameter  $\nu$  are also shown, always in the helicity  
 201 frame. In this case no clear dependence on the  $J/\psi$  kinematics is visible. Also the  $\mu$  parameter  
 202 is consistent with zero everywhere. Although not shown here, both HERA-B and NA60 results  
 203 in the Collins-Soper reference frame give  $\lambda$  values which tend to be more negative and larger in  
 204 absolute value with respect to the ones measured in the helicity frame. This is an confirmation  
 205 of the fact that the polarization parameters have a clear dependence on the chosen frame.

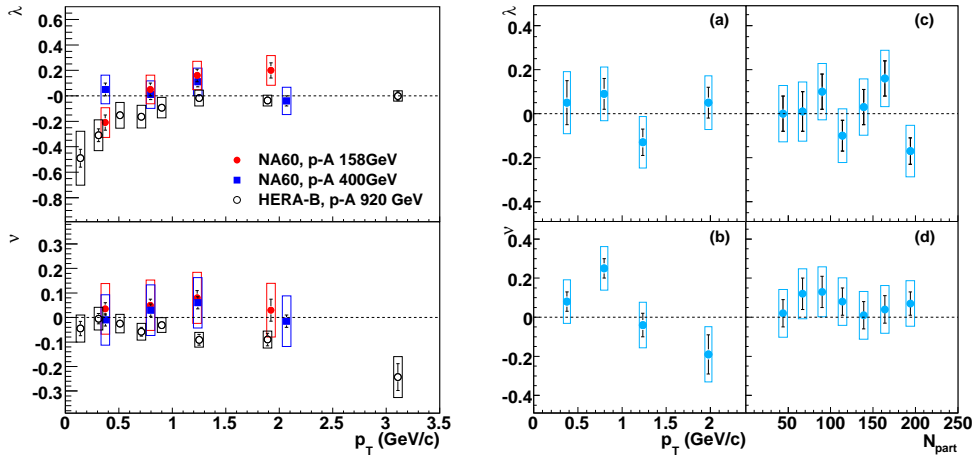


Figure 4: Left:  $J/\psi$  polarization parameters  $\lambda$  (top)  $\nu$  (bottom) and as a function of  $p_T$  in the helicity frame for p-A collisions from HERA-B and NA60. Because of a slightly different definition of the  $\nu$  parameter, with respect to HERA-B, the plotted NA60  $\nu$  values have been divided by a factor 2 with respect to those obtained from Eq. 1. Right:  $\lambda$  (a,c) and  $\nu$  (b,d) results for In-In collisions versus  $p_T$  and centrality respectively. The boxes around the points represent the total error affecting the measurement, assuming, for the NA60 points, a conservative preliminary 0.1 systematic error.

206 The HERA-B and NA60 new polarization results clearly will contribute to shed some light

207 on the polarization issue, in the attempt of describing all the available polarization measurement  
208 in a common scenario.

209 NA60 has also provided, for the first time, results on the full angular distribution of the  $J/\psi$   
210 decay products in In-In collisions. The  $\lambda$  values, in the helicity frame, do not show a dependence  
211 on the  $J/\psi$   $p_T$  as shown in Fig4 (a) and they are almost consistent with zero everywhere. Also  
212 the azimuthal coefficient  $\nu$  is rather small, pointing to a positive value only for  $p_T \sim 1$  GeV/c, as  
213 shown in Fig4 (b). The  $\lambda$  and  $\nu$  values do not present any dependence even on the centrality of  
214 the collision, as shown in Fig.4 (c,d). The pattern of these results is confirmed also if the Collins-  
215 Soper frame is adopted. In principle, it may be expected that the formation of a hot medium may  
216 affect the  $J/\psi$  polarization, as proposed in [26]. Therefore, quantitative predictions are needed,  
217 in order to clarify the observed results.

## 218 5. Conclusions

219 New NA60 results obtained in p-A collisions at 158 and 400 GeV have been presented and  
220 compared with the already existing measurements from other fixed target experiments. Cold  
221 nuclear matter effects, determined from p-A interactions, exhibit a rather strong energy and kine-  
222 matical dependence. Therefore the use of the new p-A results at 158A GeV, the same energy  
223 as the A-A data, allows a more precise definition of the expected cold nuclear matter effects in  
224 nuclear collisions. Apart from very central Pb-Pb collisions, where the anomalous suppression  
225 is still sizeable, a smaller effect with respect to previous estimates is observed. Results on  $J/\psi$   
226 polar and azimuthal parameters have also been presented for both p-A and A-A collisions.

## 227 References

- 228 [1] T. Matsui and H. Satz, *Phys. Lett.* **178** (1986) 416.  
229 [2] B. Alessandro et al. [NA50 collaboration] *Eur. Phys. J.* **48** (2006) 329.  
230 [3] B. Alessandro et al. [NA50 collaboration] *Eur. Phys. J.* **39** (2005) 335.  
231 [4] R. Araldi et al. [NA60 collaboration] *Phys. Rev. Lett.* **99** (2007) 132302  
232 [5] I. Abt et al. [HERA-B collaboration] *Eur. Phys. J.* **4** (2009) 525.  
233 [6] M.J. Leitch et al. [E866 collaboration] *Phys. Rev. Lett.* **84** (2000) 3256.  
234 [7] J. Badier et al. [NA3 collaboration] *Z. Phys.* **C20** (1983) 101.  
235 [8] E. Scomparin, these proceedings.  
236 [9] G. Usai et al. [NA60 collaboration] *Eur. Phys. J.* **43** (2005) 415.  
237 [10] B. Alessandro et al. [NA50 collaboration] *Eur. Phys. J.* **33** (2004) 31.  
238 [11] M. Kowitt et al. [E789 collaboration] *Phys. Rev. Lett.* **72** (1994) 1318.  
239 [12] M.H. Schub et al. [E789 collaboration] *Phys. Rev. D* **52** (1995) 1307.  
240 [13] T. Alexopoulos et al. [E771 collaboration] *Phys. Rev. D* **55** (1997) 3927.  
241 [14] L. Gribov et al. [E672/706 collaboration] *Phys. Rev. D* **62** (2001) 012001.  
242 [15] R. Vogt *Phys. Rev. C* **61** (2000) 035203.  
243 [16] R. Vogt *Phys. Rev. C* **71** (2005) 054902.  
244 [17] K.G. Boreskov and A.B. Kaidalov, *JETP Lett.* **D77** (2003) 559.  
245 [18] K.J. Eskola, V.J. Kolhinen and C.A. Salgado *Eur. Phys. J. C* **9** (1999) 61.  
246 [19] K.J. Eskola, H. Paukkunen and C.A. Salgado *JHEP* **0807** (2008) 102.  
247 [20] R. Araldi et al., paper in preparation  
248 [21] J.P. Lansberg *Eur. Phys. J. C* **61** (2009) 693.  
249 [22] M. Beneke et al. *Phys. Rev. D* **57** (1998) 4258.  
250 [23] E. Braaten et al. *Phys. Rev. D* **62** (2000) 094005.  
251 [24] S. Falciano et al. *Z. Phys. C* **513** (1986) 15802.  
252 [25] I. Abt et al. [HERA-B collaboration] *Eur. Phys. J.* **4** (2009) 517.  
253 [26] B.L. Ioffe and D.E. Kharzeev *Phys. Rev. C* **68** (2003) 061902.